Cell, Vol. 115, 355–367, October 31, 2003, Copyright ©2003 by Cell Press

The AAA-ATPase Cdc48/p97 Regulates Spindle Disassembly at the End of Mitosis

Kan Cao,[1,2] Reiko Nakajima,[1] Hemmo H. Meyer,[3] and Yixian Zheng[1,2,*]
[1]Department of Embryology
Carnegie Institution of Washington and Howard Hughes Medical Institute
Baltimore, Maryland 21210
[2]Department of Biology
Johns Hopkins University
Baltimore, Maryland 21218
[3]Institute of Biochemistry
ETH Hoenggerberg HPM G17.1
8093 Zurich
Switzerland

Summary

Spindle disassembly at the end of mitosis is a complex and poorly understood process. Here, we report that the AAA-ATPase Cdc48/p97 and its adapters Ufd1-Npl4, which have a well-established role in membrane functions, also regulate spindle disassembly by modulating microtubule dynamics and bundling at the end of mitosis. In the absence of p97-Ufd1-Npl4 function, microtubules in *Xenopus* egg extracts remain as monopolar spindles attached to condensed chromosomes after Cdc2 kinase activity has returned to the interphase level. Consequently, interphase microtubule arrays and nuclei are not established. Genetic analyses of Cdc48, the yeast homolog of p97, reveal that Cdc48 is also required for disassembly of mitotic spindles after execution of the mitotic exit pathway. Furthermore, Cdc48/p97-Ufd1-Npl4 directly binds to spindle assembly factors and regulates their interaction with microtubules at the end of mitosis. Therefore, Cdc48/p97-Ufd1-Npl4 is an essential chaperone that regulates transformation of the microtubule structure as cells reenter interphase.

Introduction

During cell division, the microtubule (MT) cytoskeleton undergoes cyclic transformations between a long interphase array of MTs and a highly dynamic mitotic spindle. Understanding this morphological transformation is key to deciphering the mechanism of cell division. In both interphase and mitosis, the plus ends of MTs exhibit dynamic instability characterized by abrupt switches between persistent growth and shrinkage. Studies have shown that an increased catastrophe frequency and a decreased rescue frequency contribute to spindle assembly (Cassimeris, 1999; Desai and Mitchison, 1998). The changes in dynamic instability are brought about by the cyclin-dependent kinase (Cdk) activity that promotes a phosphorylation cascade in mitosis (Belmont et al., 1990; Gliksman et al., 1992, 1993; Verde et al., 1990, 1992; Zhai et al., 1996). Recent studies show that spindle assembly requires another regulatory pathway controlled by the small GTPase Ran (Carazo-Salas et al., 1999; Kalab et al., 1999; Wilde and Zheng, 1999). The RanGTP gradient produced by condensed chromosomes (Kalab et al., 2002) promotes MT nucleation, organization, and stabilization in mitosis, thereby ensuring spindle assembly toward the chromosomes (Carazo-Salas et al., 2001; Wilde et al., 2001).

Although much is known about spindle assembly, the mechanism of spindle disassembly after mitosis has remained obscure. Consequently, it is not clear how the highly dynamic and relatively short mitotic MTs are relaxed into relatively stable and long interphase MT arrays. MT dynamics are regulated by a diverse array of proteins including MT stabilizing and destabilizing factors, as well as MT nucleators (Desai and Mitchison, 1998). The phosphorylation states of these proteins have been implicated in regulating their activities (McNally, 1996). A prevailing idea is that at the end of mitosis the degradation of cyclin B leads to the downregulation of Cdc2 kinase activity and a cascade of dephosphorylation events. As a result, spindle assembly factors are dephosphorylated, which leads to changes in MT dynamics and spindle disassembly (Desai and Mitchison, 1998). Although recent efforts have led to elegant elucidation of the mitotic exit network (MEN) that inactivates Cdc2 kinase (Bardin and Amon, 2001; Jensen et al., 2002), it is unclear whether Cdc2 inactivation alone is sufficient for regulating spindle disassembly at the end of mitosis. Since spindle disassembly has to be coordinated with many other morphological transformations such as nuclear envelope reformation and cytokinesis, regulatory controls in addition to Cdc2 inactivation and protein dephosphorylation are likely to exist.

Cdc48/p97 is an essential and highly conserved protein of the AAA-ATPase family. Like other proteins in this family, it uses ATPase activity to unfold proteins or to dissociate proteins from large cellular structures (Lupas and Martin, 2002). Interestingly, the *Saccharomyces cerevisiae CDC48* was first isolated as a cell division cycle gene (Moir et al., 1982). Certain *cdc48* mutants arrest with large budded cells and medium size mitotic spindles (Frohlich et al., 1991). However, studies thus far have only shown that Cdc48/p97 together with various adapters regulate diverse membrane-related functions (Bays and Hampton, 2002; Hetzer et al., 2001; Jarosch et al., 2002a; Meyer et al., 2000; Tsai et al., 2002).

The Ufd1-Npl4 heterodimer is one type of adaptor for Cdc48/p97 (Meyer et al., 2000). The Cdc48/p97-Ufd1-Npl4 complex has been implicated in functions such as the assembly of nuclear envelopes (Hetzer et al., 2001), the dissociation of ER proteins into the cytosol (Bays et al., 2001; Braun et al., 2002; Jarosch et al., 2002b; Ye et al., 2001), and the dissociation of a membrane-tethered transcription factor from its binding partner that is also tethered on the membrane (Hitchcock et al., 2001; Rape et al., 2001). Furthermore, some functions of Cdc48/p97-Ufd1-Npl4 are linked to the ubiquitin and/or

*Correspondence: zheng@ciwemb.edu

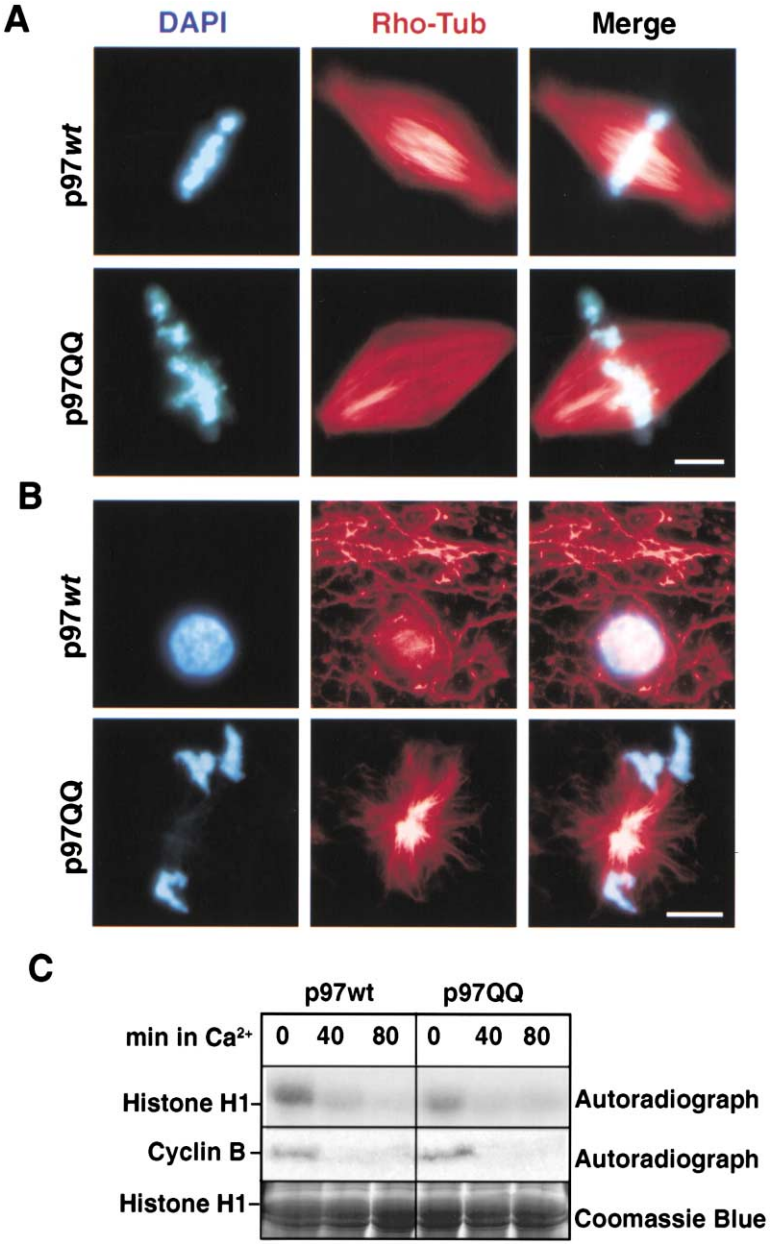

Figure 1. p97 in Spindle Disassembly

(A) p97 is not required for spindle assembly. *Xenopus* sperm were added to CSF-egg extracts in the presence of either wild-type (p97wt) or mutant (p97QQ) p97. Spindle assembly occurred with similar efficiencies in both p97wt and p97QQ treated egg extracts. Examples of the spindles are shown.

(B) p97 is required for forming interphase nuclei and MT arrays. The extracts in (A) were induced to enter interphase by Ca^{2+}. MT and nuclear structures were assayed 0, 40, or 80′ later. Shown are examples of 80′ after Ca^{2+} addition. p97QQ completely blocked the formation of interphase nuclei and MT arrays. The DNA and MTs in (A) and (B) were labeled by DAPI and rhodamine tubulin, respectively. Scale bars in (A) and (B) are equal to 10 μm.

(C) p97 is not required for Cdc2 inactivation. ^{35}S-methionine labeled cyclin B translated in vitro (Promega) was added to the reactions in (B). Degradation of cyclin B was followed by autoradiography. Cdc2 kinase activity in the reactions in (B) was assayed at 0, 40, and 80′ after Ca^{2+} addition using histone H1 as substrate.

proteasome system(s), although the detailed mechanisms are unclear (Bays and Hampton, 2002).

The finding that the Cdc48/p97-Ufd1-Npl4 complex acts as a chaperone to assist protein dissociation from a large cellular structure such as ER raises an interesting possibility that this complex could also assist spindle disassembly. A role in spindle disassembly could explain the cell cycle arrest phenotype observed in certain *cdc48* mutants (Moir et al., 1982). Using *Xenopus* egg extracts and yeast, we demonstrate that Cdc48/p97-Ufd1-Npl4 regulates spindle disassembly by modulating MT dynamics and bundling at mitotic exit. This function of Cdc48/p97-Ufd1-Npl4 is required in addition to Cdc2 inactivation. We present evidence that this complex regulates spindle disassembly by modulating the interaction between certain spindle assembly factors and MTs at the end of mitosis.

Results

Xenopus p97 Is Required for Establishing Interphase MT Arrays after Mitotic Exit

Cytosolic extracts from *Xenopus laevis* eggs (Murray, 1991) have proved suitable to study microtubule dynamics and spindle assembly. To determine whether the *Xenopus* p97 ATPase regulates spindle disassembly, we used a dominant-negative form of p97 (p97QQ), which blocks ATP hydrolysis (Ye et al., 2001), to interfere with p97 function. We found that both p97QQ and wild-type p97 (p97wt) did not perturb normal spindle assembly in cytostatic factor (CSF) arrested egg extracts (Figure 1A). We then induced the extracts to enter interphase by adding Ca^{2+}, which led to a decrease in Cdc2 kinase activity as assayed by histone H1 phosphorylation and by cyclin B degradation in extracts treated by p97QQ

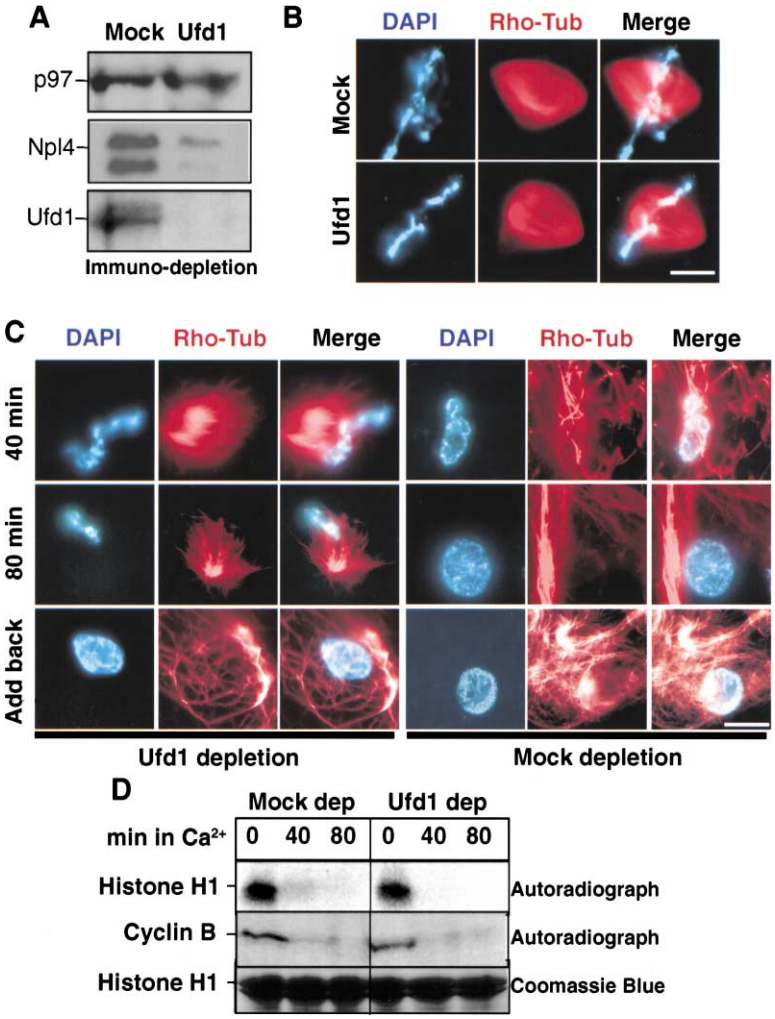

Figure 2. Ufd1-Npl4 in Spindle Disassembly

(A) Immunodepletion of Ufd1 led to codepletion of Npl4. The reduction of p97 was not noticeable because p97 is in excess of Ufd1-Npl4.

(B) Ufd1-Npl4 is not required for spindle assembly. Spindle assembly proceeded with a similar efficiency in both mock-depleted and Ufd1-Npl4-depleted extracts. Shown are examples of spindles.

(C) Ufd1-Npl4 is required for forming interphase nuclei and MT arrays. Spindles were assembled in the mock-depleted extract, the Ufd1-Npl4-depleted extract, and the Ufd1-Npl4-depleted egg extract supplemented with purified Ufd1-Npl4. The egg extracts were then induced to exit mitosis by Ca^{2+}. DNA and MTs were assayed 40 and 80′ after Ca^{2+} addition. Depletion of Ufd1-Npl4 blocked the formation of interphase nuclei and MT arrays. Adding purified Ufd1-Npl4 to the depleted extracts rescued the defects (images from 80′ after Ca^{2+} addition are shown for the add back). Scale bars in (B) and (C) are equal to 10 μm.

(D) Ufd1-Npl4 is not required for Cdc2 inactivation. Cdc2 kinase activity and cyclin B degradation in the reactions in (C) were assayed 0, 40, or 80′ after Ca^{2+} addition.

or p97wt (Figure 1C). Therefore, p97 is not required for the downregulation of Cdc2 kinase activity at mitotic exit. However, while spindle disassembly and formation of interphase nuclei occurred in the presence of p97wt (Figure 1B), both MTs and chromosomes remained in mitotic states in the presence p97QQ (Figure 1B). Thus, p97 is required for the formation of interphase MT arrays and nuclei.

Ufd1-Npl4 Is Essential for Establishing Interphase MT Arrays

We next examined whether the p97 adaptor complex, Ufd1-Npl4 (Meyer et al., 2000), is required for the transformation of mitotic spindles into the interphase MT array. The function of Ufd1-Npl4 was inhibited by either Ufd1 antibody addition or immunodepletion (Hetzer et al., 2001; Meyer et al., 2000). Since both approaches gave the same results, we show only the results for antibody depletion. Immunodepletion of Ufd1 led to codepletion of Npl4 and over 90% reduction of Ufd1-Npl4 from the extracts (Figure 2A). However, since p97 is much more abundant than Ufd1 and Npl4, there was no appreciable reduction of p97 in the Ufd1-Npl4 depleted extracts (Figure 2A). We carried out spindle assembly and disassembly reactions using the mock-depleted extract, the Ufd1-Npl4-depleted extract, or the Ufd1-Npl4-depleted extract supplemented with purified Ufd1-Npl4. Depleting Ufd1-Npl4 did not inhibit spindle assembly (Figure 2B). After Ca^{2+} addition, Cdc2 kinase activity returned to interphase levels (Figure 2D). However, despite the interphase levels of cyclin B and Cdc2 kinase activity, MTs in the Ufd1-Npl4-depleted extract remained as either half spindles or short asters with condensed chromosomes attached (Figure 2C). In contrast, spindles in the mock-depleted extract or the Ufd1-Npl4-depletion/add-back extract proceeded into interphase as characterized by the formation of interphase nuclei and MT arrays (Figure 2C). Thus, the Cdc48/p97-Ufd1-Npl4 complex is required for spindle disassembly at the end of mitosis.

The p97-Ufd1-Npl4 Complex Directly Regulates the Formation of Interphase MT Arrays

Since the p97-Ufd1-Npl4 complex is required for nuclear envelope formation (Hetzer et al., 2001), blocking its function would block chromosome decondensation and nuclei formation at the end of mitosis. We reasoned that p97-Ufd1-Npl4 could directly regulate the formation of interphase nuclei and MT arrays. Alternatively, the presence of condensed chromosomes in the extracts could

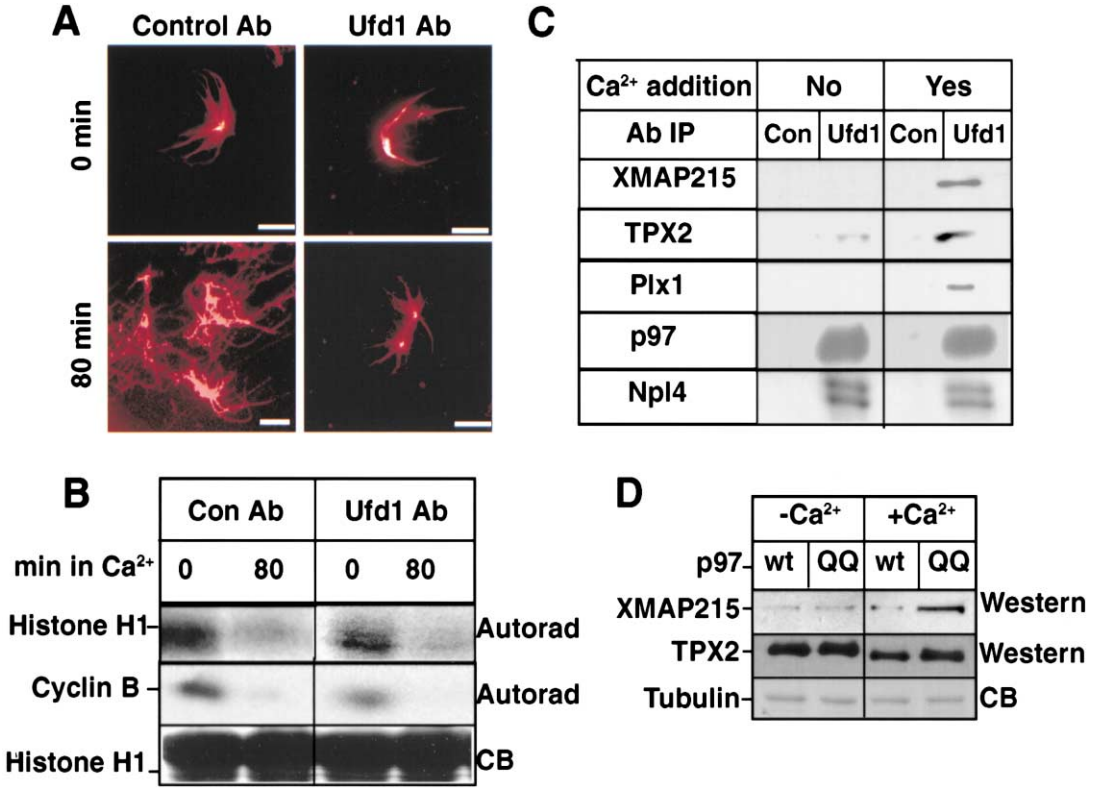

Figure 3. p97-Ufd1-Npl4 Regulates MTs at Mitotic Exit

(A) Isolated centrosomes were added to CSF-egg extracts containing either control or Ufd1 antibody to nucleate MT polymerization. The egg extracts were then induced to enter interphase by Ca^{2+}. MTs assembled in these egg extracts were analyzed 0 or 80′ after Ca^{2+} addition. Ufd1 antibody inhibited the formation of long interphase MT arrays. Scale bars are equal to 5 μm.

(B) Cdc2 kinase activity and cyclin B degradation in (A) were assayed 0 and 80′ after Ca^{2+} addition. Both control antibody (Con Ab) and Ufd1 antibody-treated egg extracts entered interphase. CB, Coomassie blue staining of histone H1.

(C) p97-Ufd1-Npl4 interacts with XMAP215, TPX2, and Plx1 at mitotic exit. Ufd1 antibody (Ufd1) or control IgG (Con) was used to immunoprecipitate the p97-Ufd1-Npl4 complex from CSF *Xenopus* egg extracts that were incubated at room temperature for 30′ in the presence or absence of Ca^{2+}. The immunoprecipitates were probed with antibodies against XMAP215, TPX2, Plx1, p97, and Npl4.

(D) p97 reduces binding of XMAP215 and TPX2 to MTs at the end of mitosis. Taxol was added to CSF extracts treated with p97wt or p97QQ to stimulate MT assembly. After triggering mitotic exit with Ca^{2+} or control buffer, MTs were sedimented through a glycerol cushion and analyzed by SDS-PAGE and Coomassie blue staining (CB). The amounts of MT-associated XMAP215 and TPX2 were determined by Western blotting.

block the formation of interphase MT arrays. To differentiate between the two possibilities, we added mammalian centrosomes instead of sperm to CSF-egg extracts to induce the formation of MT asters. The function of p97-Ufd1-Npl4 was blocked by p97QQ, by Ufd1 antibody addition, or by immunodepletion of Ufd1-Npl4. After mitotic MT asters were formed, the extracts were induced to enter interphase by Ca^{2+} addition. Since inhibition of p97-Ufd1-Npl4 by all three approaches gave similar results, we present the experiments where Ufd1 antibody was added. In control reactions, MTs successfully made the transition from short mitotic asters into long interphase networks. However, when the function of p97-Ufd1-Npl4 was blocked, the MTs remained as short asters despite the interphase levels of Cdc2 kinase activity (Figures 3A and 3B). Thus, p97-Ufd1-Npl4 directly regulates the MT cytoskeleton at mitotic exit.

The p97-Ufd1-Npl4 Complex Binds and Regulates Spindle Assembly Factors at the End of Mitosis

The mitotic spindle is a complex protein assemblage whose disassembly requires an orderly dissociation and reorganization of many MT binding proteins, motors, and protein kinases. Since p97-Ufd1-Npl4 can dissociate proteins from ER membranes, we reasoned that this complex might also assist protein dissociation from the mitotic spindle at the end of mitosis. To test this, we first asked whether p97-Ufd1-Npl4 could interact with spindle assembly factors at the end of mitosis. We used the Ufd1 antibody to immunoprecipitate p97-Ufd1-Npl4 from either CSF-egg extracts or CSF-egg extracts that had been induced to exit mitosis by Ca^{2+} addition and then screened nine spindle assembly factors for their interactions with p97-Ufd1-Npl4 (see Experimental Procedures). We found that three spindle assembly factors, XMAP215, TPX2, and Plx1, were coimmunoprecipitated with p97-Ufd1-Npl4 from the CSF-egg extract that was treated with Ca^{2+} for 30′ (Figure 3C). XMAP215 and TPX2 are MT binding proteins (Gruss et al., 2001, 2002; Shirasu-Hiza et al., 2003; Wittmann et al., 2000), while Plx1 is a spindle-associated Polo-like kinase (Nigg, 1998). These interactions were specifically regulated at mitotic exit because the signal was either decreased (TPX2) or not detectable (XMAP215 and Plx1) in the

CSF-egg extracts treated with control buffer (Figure 3C). Thus, p97-Ufd1-Npl4 binds to certain spindle assembly factors at mitotic exit.

Next, we determined whether p97-Ufd1-Npl4 could regulate the interaction between the spindle assembly factors and MTs at the end of mitosis. Taxol was used to stimulate MT polymerization in CSF-extracts treated with either p97wt or p97QQ followed by Ca^{2+} addition to trigger mitotic exit. Since we could not reliably detect Plx1 binding to taxol-stabilized MTs in CSF-extracts, we focused on studying the binding of XMAP215 and TPX2 to MTs. Western blotting showed that similar amounts of XMAP215 and TPX2 bound to MTs in CSF-extracts treated with either p97wt or p97QQ (Figure 3D). In contrast, treatment with p97QQ caused increased binding of both XMAP215 and TPX2 to MTs compared to p97wt treatment after mitotic exit (Figure 3D). Thus, p97-Ufd1-Npl4 regulates the binding of XMAP215 and TPX2 to MTs at the end of mitosis.

The p97-Ufd1-Npl4 Complex Regulates MT Dynamics at the End of Mitosis

TPX2 is required for MT nucleation and bundling in mitosis (Gruss et al., 2001; Schatz et al., 2003), whereas XMAP215 can act as a MT-destabilizing factor (Breugel et al., 2003; Shirasu-Hiza et al., 2003). Therefore, increased binding of TPX2 and XMAP215 to MTs at mitotic exit due to inhibition of p97-Ufd1-Npl4 could promote mitotic MT bundling and dynamics, thereby blocking spindle disassembly. Indeed, we observed persistent spindle-like MT bundles in egg extracts that had exited mitosis in the absence of p97-Ufd1-Npl4 function (Figures 1 and 2).

To determine whether and how p97-Ufd1-Npl4 regulates MT dynamics, we used time-lapse fluorescence microscopy to measure the dynamics of individual MTs in the CSF extracts, the control IgG-treated CSF extracts that entered interphase, or the Ufd1 antibody-treated CSF extracts that entered interphase. The CSF extracts had high levels of cyclin B and Cdc2 kinase activity, while the extracts that entered interphase had low levels of cyclin B and Cdc2 kinase activity (data not shown). As expected, interphase entry led to persistent MT growth in the control-IgG treated extracts, while MTs in the CSF-extract exhibited frequent transitions from growth to shrinkage (Figures 4A and 4B). Interestingly, MTs in the Ufd1 antibody-treated extract also exhibited frequent transitions from growth to shrinkage, despite low levels of Cdc2 kinase activity (Figures 4A and 4B).

The parameters of MT dynamics were determined in three different extracts as described previously (Wilde et al., 2001). We found that although the Ufd1 antibody-treated extracts had interphase levels of Cdc2 kinase activity, their MTs exhibited similar catastrophe and rescue frequencies as those of the CSF extracts. In contrast, in the control IgG-treated extracts, the MTs exhibited persistent growth with a 10-fold lower catastrophe frequency compared to the CSF-extracts or the Ufd1 antibody-treated extracts (Table 1). We also noticed that MTs in the Ufd1 antibody-treated extracts exhibited $\sim$2-fold higher pausing frequency during growth than MTs in the other two egg extracts. Thus, p97-Ufd1-Npl4 regulates MT catastrophe and pausing at mitotic exit.

Cdc48 Is Required for Spindle Disassembly in Yeast

To determine the in vivo function of p97 on the MT cytoskeleton, we studied a p97 homolog, Cdc48, in *Saccharomyces cerevisiae*. Since the cold sensitive mutant allele *cdc48-1* arrests with large budded cells, undivided nuclei, and medium size spindles (Frohlich et al., 1991), Cdc48 may play a role in spindle disassembly. We obtained a heat-sensitive allele of *CDC48*, *cdc48-3*, which was isolated as an intragenic suppressor of the original cold sensitive mutation *cdc48-1* (Latterich et al., 1995; Moir et al., 1982). Analyses of MT structures during a complete cell cycle in both *cdc48-3* and its wild-type control strains at either the permissive (23°C) or the restrictive temperature (37°C) revealed that spindle assembly and disassembly progressed normally at 23°C (data not shown). However, at 37°C in *cdc48-3* cells, the spindles first elongated, but instead of disassembling as in the *CDC48* strain, they collapsed into medium length spindles, which then persisted (Figures 5A and 5B). Thus, Cdc48 is required for spindle disassembly.

Cdc48 Is Required for Spindle Disassembly after Clb2 Degradation

Since Cdc48 is required for degrading certain ER proteins, it might be required for degrading Clb2, the yeast cyclin B, at mitotic exit. If so, the spindle disassembly defects observed in *cdc48-3* cells would be caused by failure to degrade cyclin B. Indeed, we found that Clb2 was not degraded in the *cdc48-3* cells at 37°C (Figure 6B), which is consistent with a previous report (Dai and Li, 2001).

However, since the Cdc48/p97-Ufd1-Npl4 complex is not required for cyclin B degradation in *Xenopus* egg extracts (Figures 1 and 2), the lack of Clb2 degradation in *cdc48-3* cells could be caused by the mitotic checkpoint response triggered by spindle disassembly defects. To test this, we deleted the checkpoint genes *MAD2* and *BUB2* (Hoyt, 2000) either individually or together in *CDC48* and *cdc48-3* strains. These strains were arrested in G1 with α factor at 23°C. After release from α factor, the cells were shifted to 37°C and sampled at 20–30′ intervals to determine the level of Clb2 and spindle morphology.

By 180′ at 37°C, the *cdc48-3*, *cdc48-3mad2*Δ, *cdc48-3bub2*Δ, and *cdc48-3mad2*Δ*bub2*Δ strains arrested with large-budded cells containing medium length spindles that had collapsed from elongated spindles (Figure 6A and Supplemental Figure S1 available at http://www.cell.com/cgi/content/full/115/3/355/DC1). As cells exited mitosis, Clb2 was degraded in *CDC48*, *CDC48mad2*Δ-*bub2*Δ, and *cdc48-3mad2*Δ*bub2*Δ cells, but only partially degraded in *cdc48-3mad2*Δ and *cdc48-3bub2*Δ cells, and not degraded at all in *cdc48-3* cells (Figure 6B). To visualize spindle disassembly, we integrated GFP-Tub1 into *CDC48mad2*Δ*bub2*Δ and *cdc48-3mad2*-Δ*bub2*Δ strains. Time-lapse fluorescence microscopy showed that spindles in both strains elongated similarly. However, while spindles in *CDC48 mad2*Δ*bub2*Δ cells disassembled, spindles in *cdc48-3mad2*Δ*bub2*Δ cells collapsed (Figure 6C). Fixed time-point experiments suggested that the collapsed spindle persisted for at least an hour. Since Clb2 is degraded in *cdc48-3mad2*Δ-

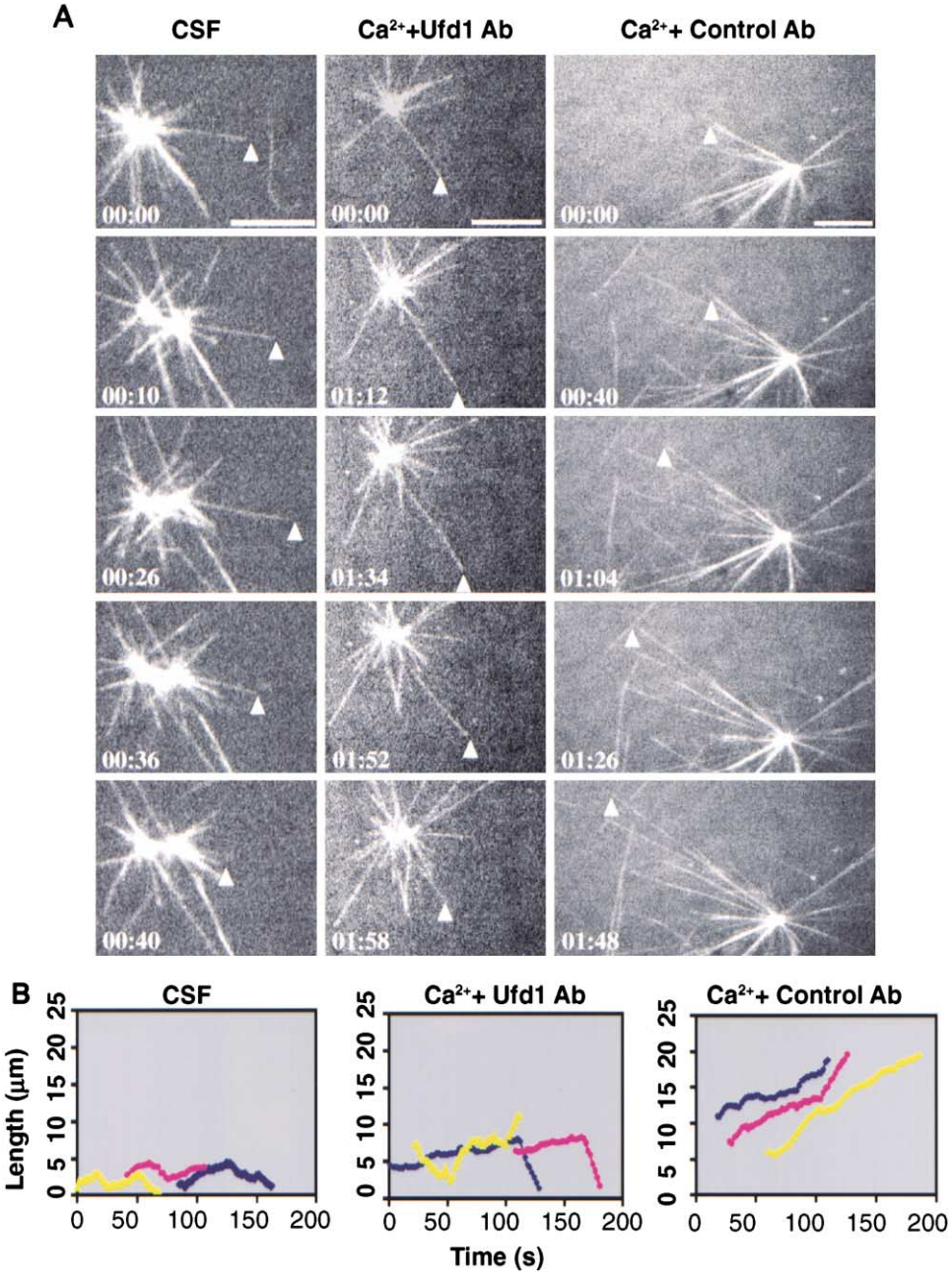

Figure 4. MT Dynamics

(A) Representative time-lapse sequences of MTs in CSF-egg extracts (CSF), CSF-egg extracts that were induced to enter interphase by adding Ca^{2+} in the presence of Ufd1 antibody (Ca^{2+} + Ufd1 Ab) or control antibody (Ca^{2+} + Control Ab). Arrowheads point to tips of MTs that undergo growth or shrinkage. Times are in min:sec. Scale bars are equal to 10 μm.

(B) Three representative MT-lifetime graphs (in three different colors) from each of the three conditions in (A).

*bub2*Δ cells that arrested with collapsed spindles (Figure 6B), Cdc48 is required for spindle disassembly after Clb2 degradation. Inactivating Cdc48 after proper spindle elongation and nuclear division also blocked spindle disassembly in *cdc48-3* cells (Supplemental Figure S2 available on *Cell* website). Thus, the spindle disassembly defect in *cdc48-3* cells was not caused by possible defects in spindle elongation or nuclear division. In addition, since the temperature sensitive mutation of Npl4, *npl4-2*, also has defects in spindle disassembly (Supplementary Figure S3 available at *Cell* website), we suggest that Cdc48-Ufd1-Npl4 regulates spindle disassembly in yeast.

Cdc48 Binds and Regulates the Degradation of Cdc5 and Ase1 at the End of Mitosis

Cdc48 binds to ER proteins and mediates their degradation by the 26 S proteasome (Bays et al., 2001; Braun

Table 1. Summary of MT Dynamic Analyses

Exps	Extracts	Vg (μm min^{-1})	Vs (μm min^{-1})	fcat (events per s)	fres (events per s)	fpg (events per s)	fps (events per s)	N
	CSF	7.2 ± 3.0	14.2 ± 6.0	0.042	0.033	0.020	0.030	16
1	Ufd1 + Ca	11.2 ± 4.6	13.0 ± 6.7	0.042	0.038	0.040	0.035	16
	Con + Ca	8.6 ± 3.9	8.6 ± 3.1	0.004	0.040	0.017	0.040	16
	CSF	8.9 ± 3.6	11.5 ± 4.4	0.032	0.032	0.033	0.032	15
2	Ufd1 + Ca	5.6 ± 2.1	14.8 ± 6.0	0.036	0.026	0.070	0.019	20
	Con + Ca	6.4 ± 2.5	10.7 ± 5.6	0.003	0.045	0.016	0.023	15
	CSF	12.4 ± 5.4	14.2 ± 5.6	0.040	0.026	0.033	0.021	12
3	Ufd1 + Ca	8.3 ± 3.1	7.5 ± 3.1	0.030	0.019	0.050	0.029	16
	Con + Ca	8.6 ± 3.8	8.7 ± 3.8	0.004	0.043	0.026	0.021	17
	CSF	9.5 ± 4.0	13.3 ± 5.3	0.038	0.030	0.029	0.028	
Avg.	Ufd1 + Ca	8.4 ± 3.2	11.8 ± 5.3	0.036	0.028	0.053	0.024	-
	Con + Ca	7.9 ± 3.4	9.3 ± 4.2	0.0036	0.043	0.020	0.028	

Analyses were performed in three different egg extracts. Rates of MT growth (Vg) and shrinkage (Vs) are shown as means ± s.d. Frequencies of catastrophe (fcat), rescue (fres), pausing while growing (fpg), and pausing while shrinking (fps) are expressed as events per second. N represents the number of MTs measured. The values of Vg, Vs, fres, and fps are similar in all three conditions: the CSF extracts (CSF), the CSF extracts that entered interphase by Ca^{2+} addition in the presence of either Ufd1 antibody (Ufd1 + Ca) or control antibody (Con + Ca). However, the fcat is ten-fold lower in Con + Ca than in CSF and Ufd1 + Ca, while fpg is two-fold higher in Ufd1 + Ca than in CSF and Con + Ca.

et al., 2002; Jarosch et al., 2002b; Rabinovich et al., 2002; Ye et al., 2001). We reasoned that Cdc48 might use a similar mechanism in assisting spindle disassembly in yeast. Consistent with this idea, Cdc5 (the yeast homolog of Plx1) and Ase1 (a yeast MT binding protein) are ubiquitinated by the anaphase-promoting complex (APC) and are degraded by the proteasome at the end of mitosis (Cheng et al., 1998; Juang et al., 1997; Pellman et al., 1995). Importantly, while a nondegradable Ase1 delays spindle disassembly (Juang et al., 1997), the nondegradable Cdc5 or constitutively active Plx1 causes multiple mitotic defects including chromosome segregation and cytokinesis (Qian et al., 1999; Song and Lee, 2001). Thus, Cdc48 might regulate spindle disassembly by binding to Cdc5 and Ase1 and mediating their degradation.

To test the role of Cdc48 in Cdc5 degradation, Myc-tagged Cdc5 was expressed in *CDC48*, *cdc48-3*, *CDC48bub2*Δ*mad2*Δ, and *cdc48-3mad2*Δ*bub2*Δ strains. The strains were first arrested in G1 at 23°C, and then released from G1 at 37°C to inactivate Cdc48 in the mutants. Western blotting showed that both Cdc5 and Clb2 were degraded at the end of mitosis in *CDC48* and *CDC48bub2*Δ*mad2*Δ cells (Figure 7A). Consistent with our earlier finding, Clb2 was also degraded in *cdc48-3bub2*Δ*mad2*Δ cells, but not in *cdc48-3* cells (Figure 7A). In contrast, Cdc5 was not degraded in either *cdc48-3* or *cdc48-3bub2*Δ*mad2*Δ cells (Figure 7A). Immunoprecipitation of VSV-tagged Cdc48 showed that Cdc5 interacted with Cdc48 (Figure 7B). Therefore, Cdc48 binds to Cdc5 and is required for its degradation at the end of mitosis.

Since Ase1 is degraded after mitotic exit in the subsequent G1 phase, we tested whether Cdc48 is required for degrading Ase1 in G1 using a method described previously (Juang et al., 1997). Myc-tagged Ase1 was expressed from the *GAL1* promoter in *CDC48* and *cdc48-3* strains. Western blotting showed that after turning off the *GAL1* promoter, Myc-Ase1 was rapidly degraded in *CDC48*, but not in *cdc48-3* cells in G1 (Figure 7C). Interestingly, *CDC48* cells accumulated less Myc-Ase1 than *cdc48-3* cells at 37°C, suggesting that Cdc48 also prevented accumulation of excess Ase1. Flow cytometry revealed that the cells were arrested in G1 with 1N DNA content (Figure 7C). Similar results were obtained in *CDC48bub2*Δ*mad2*Δ and *cdc48-3mad2*Δ*bub2*Δ cells (data not shown). Furthermore, immunoprecipitation of VSV-tagged Cdc48 showed that Cdc48 interacted with Ase1 (Figure 7D). Thus, Cdc48 interacts with Ase1 and mediates its degradation after mitotic exit.

Discussion

Cdc48/p97-Ufd1-Npl4 Regulates Spindle Disassembly at the End of Mitosis

At the end of mitosis, cyclin B degradation and Cdc2 kinase inactivation mediated by the mitotic exit network (MEN) (Bardin and Amon, 2001; Jensen et al., 2002) lead to spindle disassembly, cytokinesis, and nuclear reformation. Since Cdc48/p97-Ufd1-Npl4 functions in proteasome-mediated protein degradation, one obvious possibility is that this complex might function in the MEN pathway to mediate the degradation of cyclin B. Surprisingly, we found that cyclin B degradation and Cdc2 inactivation did not require Cdc48/p97 in either *Xenopus* egg extracts or in yeast. Instead, Cdc48/p97 is required for spindle disassembly after execution of the MEN pathway. Our studies in *Xenopus* egg extracts suggest that Cdc48/p97-Ufd1-Npl4 regulates both MT dynamics and MT bundling at the end of mitosis, thereby leading to spindle disassembly.

Interestingly, although Cdc2 inactivation in the absence of Cdc48/p97 function blocked spindle disassembly, spindle morphology changed in both *Xenopus* egg extracts and in yeast. In *Xenopus* egg extracts, bipolar spindles collapsed into monopolar spindles or asters attached to apparently condensed chromosomes, whereas in yeast the elongated spindles collapsed into medium length spindles. Since phosphorylation of the mitotic kinesin Eg5 by Cdc2 in animal cells is required for establishing and maintaining bipolar spindles (Blangy et al., 1995), it is tempting to speculate that Cdc2 inactivation

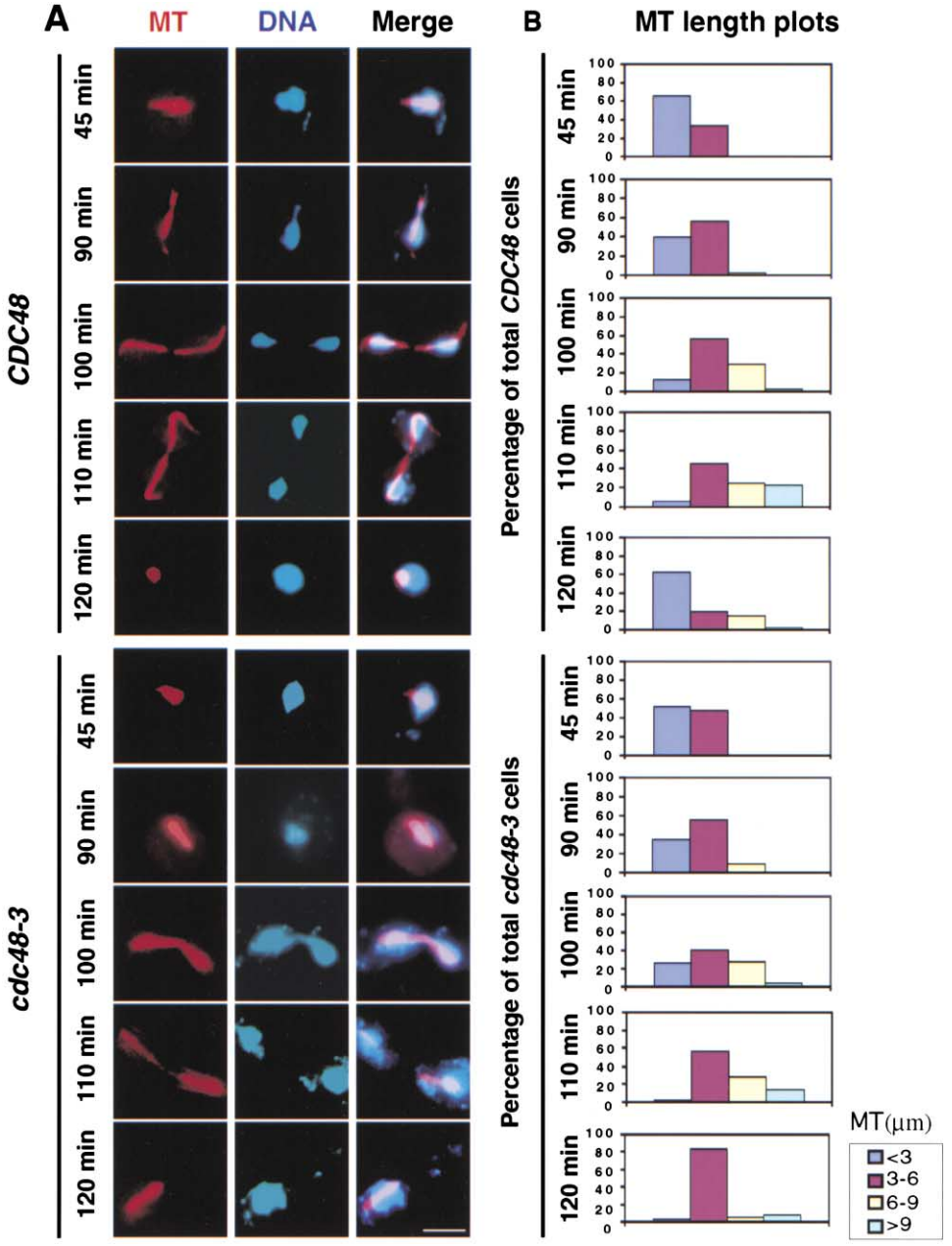

Figure 5. The *cdc48-3* Cells Arrest with Collapsed Spindles

(A) *CDC48* and *cdc48-3* cells were synchronized using α factor at 23°C. After releasing from α factor, the cultures were shifted to 37°C, and cell cycle progression was sampled by staining with Hoechst 33258 and antitubulin antibody at the indicated times. The *CDC48* cells assembled and disassembled spindles as they went through one cell cycle. However, in *cdc48-3* cells, the spindles first elongated and then collapsed into medium length spindles that persisted. Scale bar is equal to 5 μm.

(B) The spindle lengths in at least 30 cells at each time point shown in (A) were measured and plotted as histograms.

in *Xenopus* egg extracts might lead to Eg5 dephosphorylation and collapse of bipolar spindles. However, this speculation does not apply to yeast because spindle collapse occurred in *cdc48-3* cells where Clb2 was not degraded. It is interesting to note that BimC, the yeast Eg5 homolog, does not have the Cdc2 phosphorylation site that is conserved in other Eg5 homologs. Therefore, the regulation of BimC is most likely different from the other Eg5 homologs. Clearly, further analyses of the spindle-collapsing phenotype in both *Xenopus* egg extracts and in yeast should help in understanding the mechanism of spindle disassembly. Our identification of the Cdc48/p97-Ufd1-Npl4 complex as an important regulator offers a unique opportunity to study this poorly understood morphological transition.

Cdc48/p97 Binds to Spindle Assembly Factors and Regulates Their Interaction with MTs at the End of Mitosis

In *Xenopus* egg extracts, we show that Cdc48/p97-Ufd1-Npl4 interacts with XMAP215, TPX2, and Plx1 at the end of mitosis. Furthermore, inhibition of p97 func-

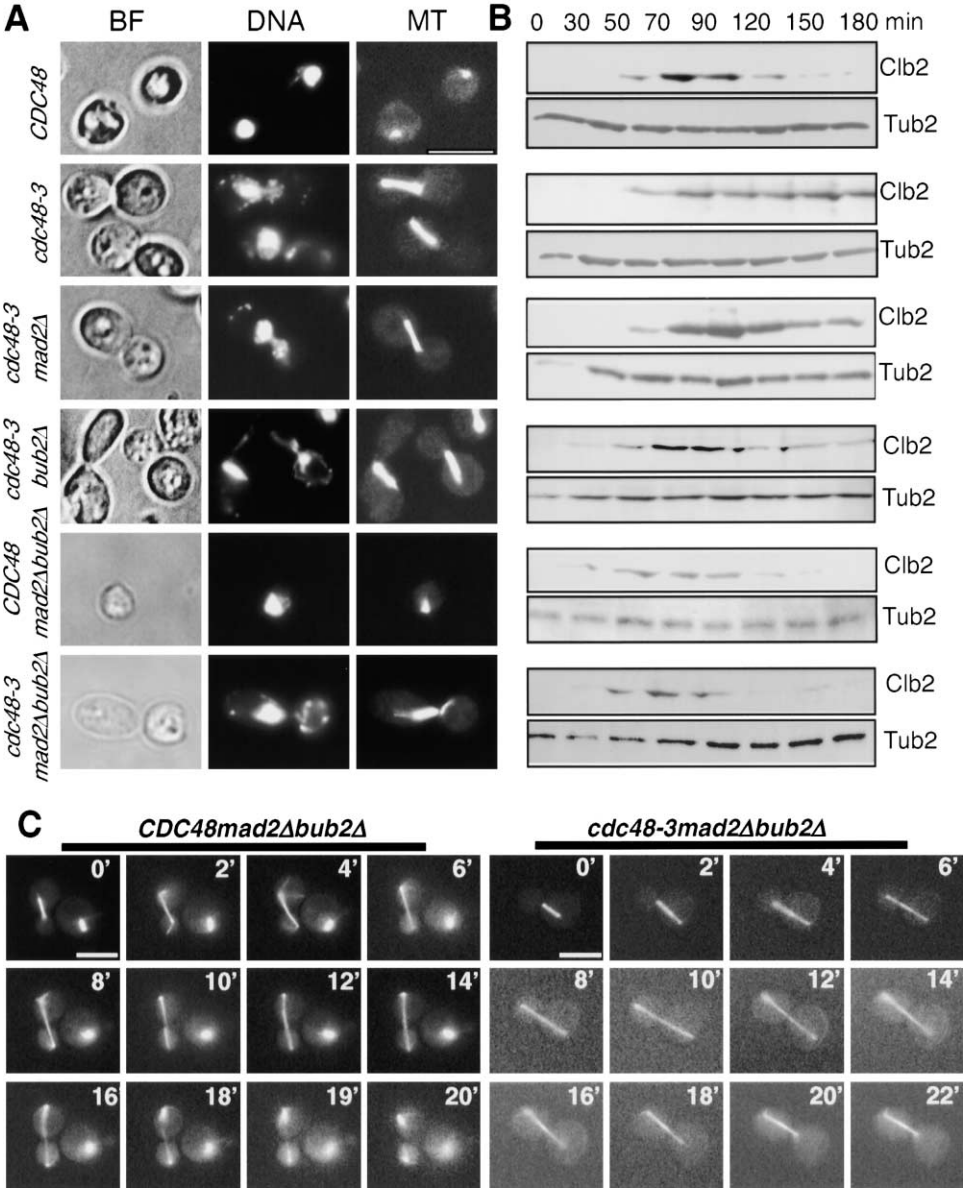

Figure 6. Cdc48 Regulates Spindle Disassembly

(A) The *CDC48*, *CDC48mad2Δbub2Δ*, *cdc48-3*, *cdc48-3mad2Δ*, *cdc48-3bub2Δ*, and *cdc48-3mad2Δbub2Δ* cells were analyzed as in Figure 5A. Shown are cells at 180 min after release from G1. While the *CDC48* and *CDC48mad2Δbub2Δ* cells underwent successful cell division and spindle disassembly, the *cdc48-3*, *cdc48-3mad2Δ*, *cdc48-3bub2Δ*, and *cdc48-3mad2Δbub2Δ* cells arrested as large budded cells with collapsed spindles. BF, brightfield. Scale bar is equal to 10 μm.

(B) Cdc48 is not required for Clb2 degradation. The same cells as in (A) were analyzed by Western blotting probing with Clb2 and Tub2 antibodies.

(C) Spindle behavior is followed by time-lapse microscopy in *CDC48mad2Δbub2Δ* or *cdc48-3mad2Δbub2Δ* cells expressing GFP-Tub1. Both strains were first arrested in G1 at 23°C and then released at 37°C. Images were captured 90′ after release from G1 at 1′ intervals. The collapsed spindles in *cdc48-3mad2Δbub2Δ* cells persisted for at least one hour. Scale bar is equal to 5 μm.

tion by p97QQ at mitotic exit leads to increased binding of XMAP215 and TPX2 to taxol-stabilized MTs. Since XMAP215 can destabilize MTs (Breugel et al., 2003; Shirasu-Hiza et al., 2003), an increased binding of XMAP215 to MTs in the absence of Cdc48/p97-Ufd1-Npl4 function may contribute to the formation of highly dynamic MTs at the end of mitosis. Furthermore, TPX2 stimulates spindle assembly by nucleating and bundling MTs (Gruss et al., 2001; Schatz et al., 2003), and by activating the mitotic kinase Aurora A in a MT-dependent manner (Tsai et al., 2003). Therefore, increased binding of TPX2 to MTs at mitotic exit due to the lack of p97 function should also contribute to the persistence of mitotic-like MT structures. We propose that Cdc48/p97-Ufd1-Npl4 binds to a subset of spindle assembly factors such as XMAP215 and TPX2, either in the cytoplasm or on the MTs at mitotic exit. This binding either sequesters the spindle assembly factors from MTs (in the case of cytosolic binding) or extracts them from MTs (if the binding occurs on MTs), thereby allowing spindle disassembly.

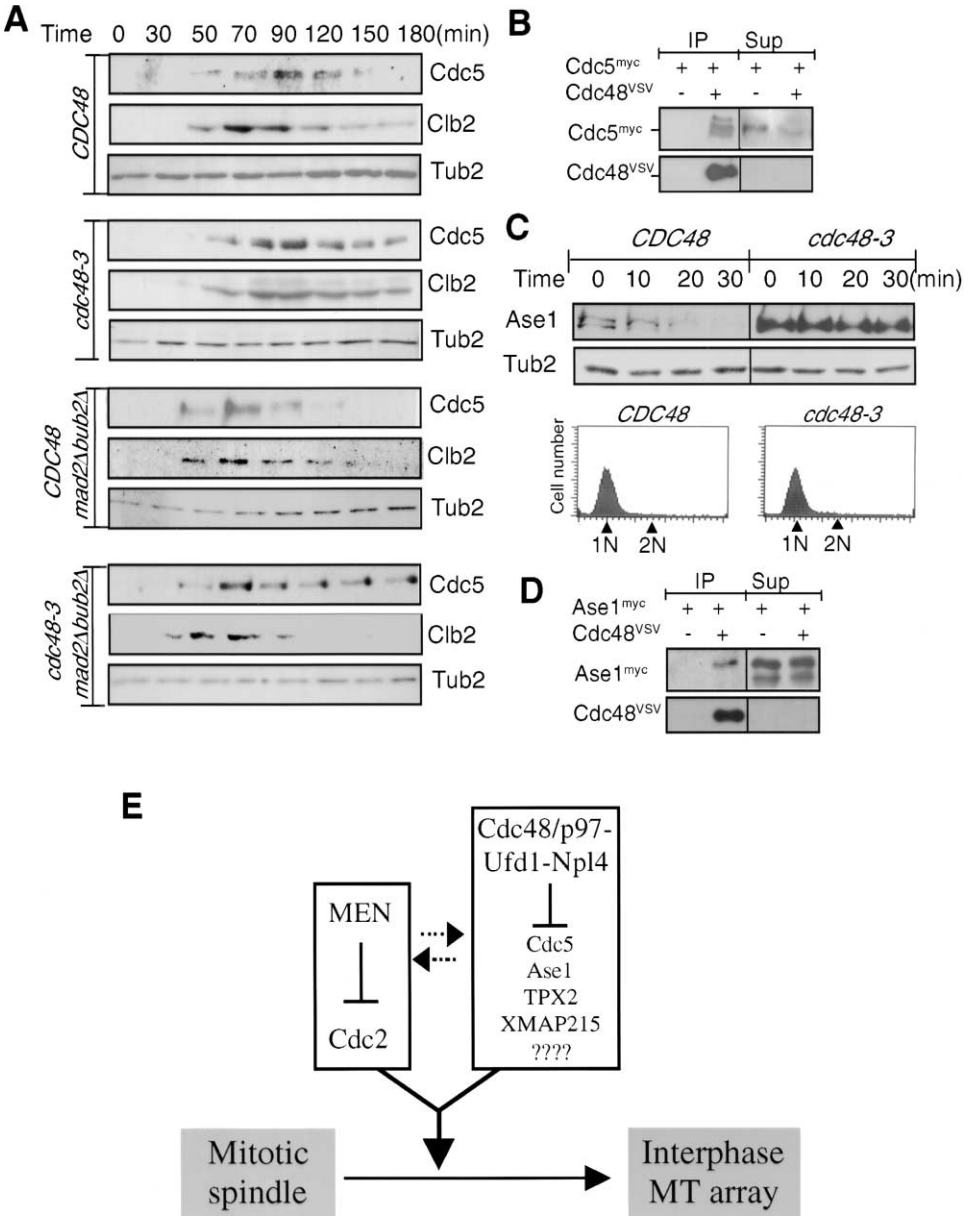

Figure 7. Cdc48 Regulates Cdc5 and Ase1

(A) Cdc48 is required for Cdc5 degradation. Western blotting analysis of Clb2, Tub2, and Myc-Cdc5 of the yeast cells sampled at indicated times after releasing from G1.

(B) Cdc48 interacts with Cdc5. Cells expressing both VSV-Cdc48 and Myc-Cdc5 or Myc-Cdc5 only were arrested in mitosis by nocodazole and released. VSV antibody pulled down Myc-Cdc5 in the presence of VSV-Cdc48 and it depleted VSV-Cdc48 from the supernatant. 37% immunoprecipitates and 2.5% of post immunoprecipitation supernatants were used for Western.

(C) Cdc48 is required for Ase1 degradation. Log phase *CDC48* and *cdc48-3* cells expressing Myc-Ase1 were synchronized in G1 at 23°C, and then shifted to 37°C. After turning off Myc-Ase1 expression, its degradation was analyzed by Western blotting. Flow cytometry showed that these cells were arrested with 1N DNA content.

(D) Cdc48 interacts with Ase1. Cells expressing both VSV-Cdc48 and Myc-Ase1 or Myc-Ase1 only were grown as in (C). VSV antibody pulled down Myc-Ase1 in the presence of VSV-Cdc48 and it depleted VSV-Cdc48. 25% (Ase1) or 5% (VSV-Cdc48) immunoprecipitates and 3% postimmunoprecipitation supernatants were used for Western.

(E) A model for spindle disassembly. At the end of mitosis, both Cdc2 inactivation mediated by the MEN pathway and the activity of Cdc48/p97-Ufd1-Npl4 are required for spindle disassembly. Cdc48/p97-Ufd1-Npl4 is required to bind to spindle assembly factors such as Cdc5, Ase1, TPX2, and XMAP215 and prevents them from promoting spindle assembly. The MEN pathway and Cdc48/p97-Ufd1-Npl4 may communicate with each other to coordinately regulate postmitotic spindle disassembly.

Consistent with the finding in *Xenopus* egg extracts, we show that Cdc48 binds to two spindle assembly factors, Ase1 and Cdc5, and is required for their degradation at the end of mitosis in yeast. Based on these studies, we propose that Cdc48/p97-Ufd1-Npl4 is required for spindle disassembly in addition to the MEN

pathway (Figure 7E). We suggest that Cdc48/p97-Ufd1-Npl4 binds to spindle assembly factors and regulates their interaction with MTs by either sequestering them from MTs or by targeting them for degradation (Figure 7E). We have identified four spindle assembly factors as targets of Cdc48/p97-Ufd1-Npl4. Considering the complexity of the spindle, additional targets of Cdc48/p97-Ufd1-Npl4 in spindle disassembly are likely to exist. Since Cdc48 regulates degradation of Cdc5, which is an activator of the MEN pathway, the Cdc48/p97-Ufd1-Npl4 pathway may negatively regulate the MEN pathway at the end of mitosis. It will be interesting to study whether the MEN pathway also regulates the activity of Cdc48/p97-Ufd1-Npl4 during spindle disassembly.

Comparing the Role of Cdc48/p97-Ufd1-Npl4 in Membrane Functions and in Spindle Disassembly

Our findings suggest that the role of Cdc48/p97-Ufd1-Npl4 on the membranes and on MTs is similar in three aspects. First, Cdc48/p97 binds to Ase1 and Cdc5 and mediates their degradation in yeast. Similar to degradation of ER-associated proteins, the degradation of both Ase1 and Cdc5 requires ubiquitination, which is mediated by APC (Cheng et al., 1998; Juang et al., 1997). Second, Cdc48/p97-Ufd1-Npl4 binds to XMAP215 and TPX2 and regulates their binding to MTs at mitotic exit in *Xenopus* egg extracts. This regulation does not appear to involve protein degradation because neither XMAP215 nor TPX2 is degraded in the egg extracts. Similarly, Cdc48/p97-Ufd1-Npl4 can also regulate dissociation of a membrane-tethered transcription factor without targeting it for degradation (Bays and Hampton, 2002; Hitchcock et al., 2001; Rape et al., 2001). Finally, although Cdc48/p97-Ufd1-Npl4 binds ubiquitin directly (Meyer et al., 2002), ubiquitination of its substrate does not seem to be a prerequisite for an interaction, since p97-Ufd1-Npl4 can also bind to an ERAD substrate prior to ubiquitination (Ye et al., 2001). Similarly, we found that Ase1, Cdc5, TPX2, XMAP215, and Plx1 that coimmunoprecipitated with Cdc48/p97 were not modified by polyubiquitin as judged by their size. One possibility is that Cdc48/p97-Ufd1-Npl4 may recognize the spindle assembly factors independent of ubiquitination. Alternatively, the spindle assembly factors may be recognized by Cdc48/p97-Ufd1-Npl4 indirectly via interactions with unidentified ubiquitinated proteins.

The findings presented in this study extend the repertoire of Cdc48/p97-Ufd1-Npl4 from regulating membrane function to spindle disassembly. Since both the MT cytoskeleton and the membrane network undergo dramatic reorganizations at the end of mitosis, Cdc48/p97-Ufd1-Npl4 may coordinate these diverse morphological transformations after cell division. Further study of how Cdc48/p97-Ufd1-Npl4 functions on membranes and on mitotic spindles should reveal whether this complex uses similar mechanisms to disassemble protein complexes from the two very different cellular structures.

Experimental Procedures

Proteins and Antibodies

Purification of p97, p97QQ, Ufd1-Npl4, and antibodies against Ufd1 (5E2), Npl4, and p97 were described (Hetzer et al., 2001; Meyer et al., 2000). For antibody addition experiments, the Ufd1 and control antibodies (Jackson Laboratories) were dialyzed against XB buffer (10 mM HEPES, [pH 7.7], 50 mM sucrose, 100 mM KCl, 0.1 mM $CaCl_2$, and 5 mM EGTA) and concentrated to 2–3 mg/ml. Antibodies against yeast Clb2, *Xenopus* XCTK2, and XKCM1 were gifts (Desai et al., 1999; Stegmeier et al., 2002; Walczak et al., 1997). Antibodies against *Xenopus* XMAP215, Plx2, TPX2, Aurora A, Aurora B, Eg5, and Incenp were raised in rabbits and affinity purified. Antibodies against yeast α-tubulin (YOL1/34), Myc-tag (9E10), and VSV-tag were from Serotec, Santa Cruz, and Sigma, respectively. Rhodamine tubulin was prepared as described (Hyman et al., 1991).

Experiments in Egg Extracts

CSF-arrested *Xenopus* egg extracts, *Xenopus* sperm, and mammalian centrosomes were prepared as described (Mitchison and Kirschner, 1986; Murray and Kirschner, 1989). Centrosomes (final $\sim 0.5 \times 10^3$ centrosomes/μl) or sperm (final $\sim$500 sperm/μl) were added to CSF extracts containing 100 μg/ml rhodamine-labeled tubulin and incubated at room temperature (RT) for 30–90′ to induce aster or spindle assembly, respectively. The egg extracts were then induced to enter interphase by adding calcium chloride (final 0.4 mM) and incubation at RT for 40–90′.

To inhibit p97, purified bacterially expressed wild-type p97 or p97QQ was added to the CSF-egg extracts to a final concentration of 0.5–0.6 mg/ml and incubated for 30′ on ice before initiating spindle assembly or MT aster formation at RT. To inhibit Ufd1-Npl4, the Ufd1 antibody or a control IgG was added to the CSF-egg extracts (final 0.5–0.6 mg/ml) and incubated for 30′ on ice before initiating reactions at RT. To deplete Ufd1-Npl4 in 100 μl of CSF-egg extracts, 40 μg of the Ufd1 antibody was used. Purified Ufd1-Npl4 complex was added back to the depleted extracts as described (Hetzer et al., 2001). Cdc2 kinase activity and cyclin B degradation were assayed as described (Felix et al., 1989).

The MT spin down experiments were carried out by adding taxol (1 μM final) to CSF extracts containing p97 or p97QQ and incubated at RT for 10′. Ca^{2+} or control buffer was added to the extracts for 30′. MTs were pelleted through a glycerol cushion and analyzed by Western blotting.

To identify p97-Ufd1-Npl4 interactors, CSF-egg extracts were treated with Ca^{2+} or control buffer for 30′ at RT. p97-Ufd1-Npl4 was immunoprecipitated from extracts using Ufd1 antibody or control IgG. The immunoprecipitates were probed with antibodies against *Xenopus* XMAP215, Plx1, TPX2, Aurora A, Aurora B, Eg5, Incenp, XCTK2, and XKCM1.

MT dynamics were measured as described (Wilde et al., 2001). Time-lapse images were recorded with a cooled CCD camera (Hamamatsu) using 750 ms exposures at 2 s (mitotic dynamics) or 5 s (interphase dynamics) intervals on a spinning disk confocal (Perkin-Elmer) microscope (Leica DMIRE2).

Yeast Experiments

Lists of yeast strains and plasmids are provided in Supplemental Tables S1 and S2 available on *Cell* website. MTs and DNA were stained with YOL1/34 and Hoechst 33258, respectively. To examine the stability of Ase1 in G1, *CDC48*, *cdc48-3, CDC48mad2Δbub2Δ*, and *cdc48-3mad2Δbub2Δ* strains containing *GAL1::ASE1*-3Myc (PB338) were grown to mid-log phase in medium containing 2% raffinose at 23°C. α-factor was added for 3 hr in the presence of 2% galactose to induce Ase1 expression. After one hour at 37°C, Ase1 expression was turned off and the Ase1 degradation time course was determined by Western blotting. Flow cytometry was used to determine DNA content of the G1-arrested cells.

To determine whether Cdc48 interacts with Ase1 and Cdc5, we used anti-VSV antibody to immunoprecipitate VSV-Cdc48 (Rape et al., 2001) from yeast strain *ura3-52trp1Δ63Leu2Δ1* expressing VSV-Cdc48, Myc-Ase1, or Myc-Cdc5. VSV-Cdc48 and Myc-Cdc5 were expressed under the control of their own promoters. Ase1 expression was under the control of *GAL1* promoter. For Ase1, cells were grown in the same manner as for Ase1 degradation experiments. For Cdc5, cells were arrested in mitosis using nocodazole and released before immunoprecipitation. The cells were lysed with glass beads in lysis buffer (50 mM Tris-HCl [pH 7.4], 50 mM KCl, 2.5 mM $MgCl_2$, 0.5% Triton X-100, and 0.1 mM DTT). The clarified lysates were

subjected to immunoprecipitation with monoclonal VSV antibody. The proteins bound to beads were analyzed by Western blotting probing with antibodies against VSV and Myc tags.

Acknowledgments

We thank Drs. R. Schekman, D. Pellman, R. Chen, A. Hoyt, A. Amon, R. Li, D. Koshland, P. Silver, A. Murray, S. Biggins, C. Walczak, K. Lee, and S. Jentsch for plasmids, antibodies, and yeast strains; Drs. R. Li, H. Yu, C. Dougherty, D. Koshland, S. Biggins, and A. Hoyt for invaluable help with yeast techniques; Drs. A. Hoyt, D. Koshland, J. Wilhelm, T. Murphy, J. Yanowitz, Q. Guo, and members of the Zheng lab for critical comments; and Dr. G. Warren for generous support. Supported by HHMI (Y.Z.), Human Frontiers Science Project, NIH, and Ludwig Institute for cancer research to Graham Warren (H.H.M.).

Received: February 4, 2003
Revised: September 9, 2003
Accepted: October 2, 2003
Published: October 30, 2003

References

Bardin, A.J., and Amon, A. (2001). MEN and SIN: what is the difference? Nat. Rev. Mol. Cell Biol. *2*, 815–823.

Bays, W.B., and Hampton, R.Y. (2002). Cdc48-Ufd1-Npl4: stuck in the middle with Ub. Curr. Biol. *12*, R366–R371.

Bays, W.B., Wilhovsky, S.K., Goradia, A., Hodgkiss-Harlow, K., and Hampton, R.Y. (2001). HRD4/NPL4 is required for the proteasomal processing of ubiquitinated ER proteins. Mol. Biol. Cell *12*, 4114–4128.

Belmont, L.D., Hyman, A.A., Sawin, K.E., and Mitchison, T.J. (1990). Real-time visualization of cell cycle-dependent changes in microtubule dynamics in cytoplasmic extracts. Cell *62*, 579–589.

Blangy, A., Lane, H.A., d'Herin, P., Harper, M., Kress, M., and Nigg, E.A. (1995). Phosphorylation by p34cdc2 regulates spindle association of human Eg5, a kinesin-related motor essential for bipolar spindle assembly in vivo. Cell *83*, 1159–1169.

Braun, S., Matuschewski, K., Rape, M., Thoms, S., and Jentsch, S. (2002). Role of the ubiquitin-selective CDC48$^{ufd1/NPL4}$ chaperone (segregase) in ERAD of OLE1 and other substrates. EMBO J. *21*, 615–621.

Breugel, M.V., Drechsel, D., and Hyman, A.A. (2003). Stu2p, the budding yeast member of the conserved Dis1/XMAP215 family of microtubule-associated proteins is a plus end-binding microtubule destabilizer. J. Cell Biol. *161*, 359–369.

Carazo-Salas, R.E., Guarguaglini, G., Gruss, O.J., Segref, A., Karsenti, E., and Mattaj, I.W. (1999). Generation of GTP-bound Ran by RCC1 is required for chromatin-induced mitotic spindle formation. Nature *400*, 178–181.

Carazo-Salas, R.E., Gruss, O.J., Mattaj, I.W., and Karsenti, E. (2001). RanGTP coordinates the regulation of microtubule nucleation and dynamics during mitotic spindle assembly. Nat. Cell Biol. *3*, 228–234.

Cassimeris, L. (1999). Accessory protein regulation of microtubule dynamics throughout the cell cycle. Curr. Opin. Cell Biol. *11*, 134–141.

Cheng, L., Hunke, L., and Hardy, C.F.J. (1998). Cell cycle regulation of the *Saccharomyces cerevisiae* polo-like kinase Cdc5p. Mol. Cell. Biol. *18*, 7360–7370.

Dai, R.M., and Li, C.H. (2001). Valosin-containing protein is a multi-ubiquitin chain-targeting factor required in ubiquitin-proteasome degradation. Nat. Cell Biol. *3*, 740–744.

Desai, A., and Mitchison, T.J. (1998). Microtubule polymerization dynamics. Annu. Rev. Cell Dev. Biol. *13*, 83–117.

Desai, A., Verma, S., Mitchison, T., and Walczak, C.E. (1999). Kin I kinesins are microtubule-destabilizing enzymes. Cell *1*, 69–78.

Felix, M.A., Pines, J., Hunt, T., and Karsenti, E. (1989). A post-ribosomal supernatant from activated Xenopus eggs that displays post-translationally regulated oscillation of its cdc2+ mitotic kinase activity. EMBO J. *8*, 3059–3069.

Frohlich, K.U., Fries, H., Rudiger, M., Erdmann, R., Botstein, D., and Mecke, D. (1991). Yeast cell cycle protein CDC48p shows full-length homology to the mammalian protein VCP and is a member of a protein family involved in secretion, peroxisome formation, and gene expression. J. Cell Biol. *114*, 443–453.

Gliksman, N.R., Parsons, S.F., and Salmon, E.D. (1992). Okadaic acid induces interphase to mitotic-like microtubule dynamic instability by inactivating rescue. J. Cell Biol. *119*, 1271–1276.

Gliksman, N.R., Skibbens, R.V., and Salmon, E.D. (1993). How the transition frequencies of microtubule dynamic instability (nucleation, catastrophe, and rescue) regulate microtubule dynamics in interphase and mitosis: analysis using a Monte Carlo computer simulation. Mol. Biol. Cell *4*, 1035–1050.

Gruss, O.J., Carazo-Salas, R.E., Schatz, C.A., Guarguaglini, G., Kast, J., Wilm, M., Bot, N.L., Vernos, I., Karsenti, E., and Mattaj, I.W. (2001). Ran induces spindle assembly by reversing the inhibitory effect of importin α on TPX2 activity. Cell *104*, 83–92.

Gruss, O.J., Wittmann, M., Yokoyama, H., Pepperkok, R., Kufer, T., Sillje, H., Karsenti, E., Mattaj, I.W., and Vernos, I. (2002). Chromosome-induced microtubule assembly mediated by TPX2 is required for spindle formation in HeLa cells. Nat. Cell Biol. *4*, 871–879.

Hetzer, M., Meyer, H.H., Walther, T.C., Cortes-Bilbao, D., Warren, G., and Mattaj, I.W. (2001). Distinct AAA-ATPase p97 complexes function in discrete steps of nuclear assembly. Nat. Cell Biol. *3*, 1086–1091.

Hitchcock, A.L., Krebber, H., Frietze, S., Lin, A., Latterich, M., and Silver, P.A. (2001). The conserved Npl4 protein complex mediates proteasome-dependent membrane-bound transcription factor activation. Mol. Biol. Cell *12*, 3226–3241.

Hoyt, M.A. (2000). Exit from mitosis: spindle pole power. Cell *102*, 267–270.

Hyman, A., Drechsel, D., Kellogg, D., Salser, S., Sawin, K., Steffen, P., Wordeman, L., and Mitchison, T. (1991). Preparation of modified tubulins. Meth. Enzymol. *196*, 478–487.

Jarosch, E., Geiss-Friedlander, R., Meusser, B., Walter, J., and Sommer, T. (2002a). Protein dislocation from the endoplasmic reticulum–pulling out the suspect. Traffic *3*, 530–536.

Jarosch, E., Taxis, C., Volkwein, C., Bordallo, J., Finley, D., Wolf, D.H., and Sommer, T. (2002b). Protein dislocation from the ER requires polyubiquitination and the AAA-ATPase Cdc48. Nat. Cell Biol. *4*, 134–139.

Jensen, S., Geymonat, M., and Johnston, L.H. (2002). Mitotic exit: delaying the end without FEAR. Curr. Biol. *12*, R221–R223.

Juang, Y., Huang, J., Peters, J., Mclaughlin, M.E., Tai, C., and Pellman, D. (1997). APC-mediated proteolysis of Ase1 and the morphogenesis of the mitotic spindle. Science *275*, 1311–1314.

Kalab, P., Pu, R., and Dasso, M. (1999). The Ran GTPase regulates mitotic spindle assembly. Curr. Biol. *9*, 481–484.

Kalab, P., Weis, K., and Heald, R. (2002). Visualization of a Ran-GTP gradient in interphase and mitotic Xenopus egg extracts. Science *295*, 2452–2456.

Latterich, M., Frohlich, K.U., and Schekman, R. (1995). Membrane fusion and the cell cycle: Cdc48p participates in the fusion of ER membranes. Cell *82*, 885–893.

Lupas, A.N., and Martin, J. (2002). AAA proteins. Curr. Opin. Struct. Biol. *12*, 746–753.

McNally, F.J. (1996). Modulation of microtubule dynamics during the cell cycle. Curr. Opin. Cell Biol. *8*, 23–29.

Meyer, H.H., Shorter, J.G., Seemann, J., Pappin, D., and Warren, G. (2000). A complex of mammalian Ufd1 and Npl4 links the AAA-ATPase, p97, to ubiquitin and nuclear transport pathways. EMBO J. *19*, 2181–2192.

Meyer, H.H., Wang, Y., and Warren, G. (2002). Direct binding of ubiquitin conjugates by the mammalian p97 adaptor complexes, p47 and Ufd1-Npl4. EMBO J. *21*, 5645–5652.

Mitchison, T.J., and Kirschner, M.W. (1986). Isolation of mammalian centrosomes. Meth. Enzymol. *134*, 261–268.

Moir, D., Stewart, S.E., Osmond, B.C., and Botstein, D. (1982). Cold

sensitive cell-division-cycle mutants of yeast: isolation, properties, and pseudoreversion studies. Genetics *100*, 547–563.

Murray, A.W. (1991). Cell cycle extracts. Methods Cell Biol. *36*, 581–605.

Murray, A.W., and Kirschner, M.W. (1989). Cyclin synthesis drives the early embryonic cell cycle. Nature *339*, 275–280.

Nigg, E.A. (1998). Polo-like kinases: positive regulators of cell division from start to finish. Curr. Opin. Cell Biol. *10*, 776–783.

Pellman, D., Bagget, M., Tu, H., and Fink, G.R. (1995). Two microtubule-associated proteins required for anaphase spindle movement in Saccharomyces cerevisiae. J. Cell Biol. *130*, 1373–1385.

Qian, Y.-W., Erikson, E., and Maller, J. (1999). Mitotic effects of a constitutively active mutant of the Xenopus polo-like kinase Plx1. Mol. Cell. Biol. *19*, 8625–8635.

Rabinovich, E., Kerem, A., Frohlich, K.U., Diamant, N., and Bar-Nun, S. (2002). AAA-ATPase p97/Cdc48, a cytosolic chaperone required for endoplasmic reticulum-associated protein degradation. Mol. Cell. Biol. *22*, 626–634.

Rape, M., Hoppe, T., Gorr, I., Kalcocay, M., Richly, H., and Jentsch, S. (2001). Mobilization of processed, membrane-tethered SPT23 transcription factor by CDC48/Ufd1/Npl4, a ubiquitin-selective chaperone. Cell *107*, 667–677.

Schatz, C.A., Santarella, R., Hoenger, A., Karsenti, E., Mattaj, I.W., Gruss, O.J., and Carazo-Salas, R.E. (2003). Importin α-regulated nucleation of microtubules by TPX2. EMBO J. *22*, 2060–2070.

Shirasu-Hiza, M., Coughlin, P., and Mitchison, T. (2003). Identification of XMAP215 as a microtubule-destabilizing factor in Xenopus egg extract by biochemical purification. J. Cell Biol. *161*, 349–358.

Song, S., and Lee, K. (2001). A novel function of *Saccharomyces cerevisiae CDC5* in cytokinesis. J. Cell Biol. *152*, 451–469.

Stegmeier, F., Visintin, R., and Amon, A. (2002). Separase, Polo kinase, the kinetochore protein Slk19, and Spo12 function in a network that controls Cdc14 localization during early anaphase. Cell *108*, 207–220.

Tsai, B., Ye, Y., and Rapoport, T.A. (2002). Retro-translocation of proteins from the endoplasmic reticulum into the cytosol. Nat. Rev. Mol. Cell Biol. *3*, 246–255.

Tsai, M.-Y., Wiese, C., Cao, K., Martin, O.C., Donovan, P.J., Ruderman, J.V., Prigent, C., and Zheng, Y. (2003). A Ran signalling pathway mediated by the mitotic kinase Aurora A in spindle assembly. Nat. Cell Biol. *5*, 242–248.

Verde, F., Labbe, J.C., Doree, M., and Karsenti, E. (1990). Regulation of microtubule dynamics by cdc2 protein kinase in cell-free extracts of Xenopus eggs. Nature *343*, 233–238.

Verde, F., Dogterom, M., Stelzer, E., Karsenti, E., and Leibler, S. (1992). Control of microtubule dynamics and length by cyclin A- and cyclin B-dependent kinases in Xenopus egg extracts. J. Cell Biol. *118*, 1097–1108.

Walczak, C., Verma, S., and Mitchison, T. (1997). XCTK2: a kinesin-related protein that promotes mitotic spindle assembly in Xenopus laevis egg extracts. J. Cell Biol. *136*, 859–870.

Wilde, A., and Zheng, Y. (1999). Stimulation of microtubule aster formation and spindle assembly by the small GTPase Ran. Science *284*, 1359–1362.

Wilde, A., Lizarraga, S.B., Zhang, L., Wiese, C., Gliksman, N.R., Walczak, C.E., and Zheng, Y. (2001). Ran stimulates spindle assembly by changing microtubule dynamics and the balance of motor activities. Nat. Cell Biol. *3*, 221–227.

Wittmann, T., Wilm, M., Karsenti, E., and Vernos, I. (2000). TPX2, A novel Xenopus MAP involved in spindle pole organization. J. Cell Biol. *149*, 1405–1418.

Ye, Y., Meyer, H.H., and Rapopport, T.A. (2001). The AAA ATPase Cdc48/p97 and its partners transport proteins from the ER into the cytosol. Nature *414*, 652–656.

Zhai, Y., Kronebusch, P.J., Simon, K.M., and Borisy, G.G. (1996). Microtubule dynamics at the G2/M transition: abrupt breakdown of cytoplasmic microtubules at nuclear envelope breakdown and implications for spindle morphogenesis. J. Cell Biol. *135*, 201–214.